



Science Arts & Métiers (SAM)

is an open access repository that collects the work of Arts et Métiers Institute of Technology researchers and makes it freely available over the web where possible.

This is an author-deposited version published in: <https://sam.ensam.eu>
Handle ID: <http://hdl.handle.net/10985/20661>

To cite this version :

DUC TAN VU, Ngac Ky NGUYEN, Eric SEMAIL - Torque Ripple Eliminations for Multiphase Nonsinusoidal Permanent Magnet Synchronous Machines - In: 2021 International Symposium on Electrical and Electronics Engineering (ISEE), Viêt Nam, 2021-04-15 - 2021 International Symposium on Electrical and Electronics Engineering (ISEE) - 2021

Any correspondence concerning this service should be sent to the repository

Administrator : scienceouverte@ensam.eu



Torque Ripple Eliminations for Multiphase Non-sinusoidal Permanent Magnet Synchronous Machines

Duc Tan Vu^{1,2}, Ngac Ky Nguyen¹, Eric Semail¹

¹Univ. Lille, Arts et Metiers Institute of Technology, Central Lille, Junia, ULR 2697 - L2EP, F-59000 Lille, France

²Thai Nguyen University of Technology, Thai Nguyen, Vietnam

Abstract—This paper is to propose a control scheme, a combination of the classical field-oriented control (FOC) technique and artificial intelligence (AI), to obtain constant torques in multiphase non-sinusoidal permanent magnet synchronous machine (PMSM) drives. Higher torque density, easier fabrication, and lower costs are several advantages of non-sinusoidal back electromotive force (back-EMF) machines over sinusoidal ones. However, multi-harmonics existing in back-EMFs possibly generate torque ripples, reducing torque quality of the drive. Therefore, in this paper, an adaptive linear neuron (ADALINE), a simple type of AI, is combined with the classical FOC technique to eliminate these torque ripples. The proposed control scheme is validated by numerical results with a seven-phase PMSM. In addition, these results are compared with an existing strategy to prove its effectiveness.

Keywords—Multiphase machine, seven-phase PMSM, non-sinusoidal back-EMF, torque ripple elimination, ADALINE, artificial intelligence.

I. INTRODUCTION

Multiphase machines have been becoming a favorable choice in applications that require high functional reliability. An increase in the number of phases ($n > 3$) gives multiphase machines more degrees of freedom for design and control. Therefore, fault tolerance, low power per phase rating, and low-ripple torque can be several advantages of multiphase machines over conventional three phase machines [1, 2].

The design requirement is relaxed as the number of phases is high. Indeed, according to the multi-reference frame theory [3], a n -phase symmetrical machine is characterized by $(n+1)/2$ (if n is odd) and $(n+2)/2$ (if n is even) characteristic planes, known as reference frames. One frame is associated with a group of harmonics. A constant torque can be ideally obtained when only a single harmonic of currents and back-EMFs exists in each reference frame (except the zero-sequence frames). Therefore, an increase in the number of phases results in more reference frames, permitting to have more harmonics in back-EMFs. Consequently, in a well-designed multiphase machine, the torque generated by non-sinusoidal back-EMFs can be constant by imposing constant d-q currents in each reference frame. Therefore, the FOC technique with classical proportional integral (PI) controllers that have been popular in industry are facilitated. This characteristic is not available in a three-phase machine. Indeed, a three-phase machine with two reference frames (including one zero-sequence frame) requires the classical constraints on sinusoidal back-EMFs and sinusoidal currents. Therefore, a multiphase machine leads to fewer constraints on design than a three-phase machine.

However, due to the imperfection of machine manufacture, non-sinusoidal back-EMFs could contain more than one harmonic per frame, conflicting the multi-reference frame theory. Negative impacts of these harmonics on current control have been discussed and solved in [4, 5]. The approach is similar to [6] for a high-speed three-phase machine drive. Nonetheless, even when current control quality is guaranteed, torque ripples still exist due to the interaction between currents and back-EMF harmonics. The vectorial approach [7], known as maximum torque per ampere (MTPA) for all phase numbers, all types of back-EMFs, and all operating modes, can be a solution to eliminate torque ripples. Time-variant current references for control by this approach require a controller whose bandwidth increases with the rotating speed. Therefore, hysteresis controllers have been chosen in [7], leading to inevitable variable switching frequencies, high switching losses, and electromagnetic compatibility problems. Another approach using ADALINES can be found in [8] in which optimal currents for non-sinusoidal multiphase PMSMs. However, the entire optimal torque is used in the learning process, making all current references have highly oscillating waveforms as in [7]. An artificial Gaussian-type radial basis function neural network has been applied to control the speed of a 5-phase drive without knowledge of accurate machine models or parameters [9]. However, this neural network (multi-layers) is more complicated than ADALINES, requiring more learning time. In addition, hysteresis-type controllers are used for the control of time-variant current references, resulting in unexpected effects as in [7]. Several control techniques, such as model predictive control [10] or pulse width modulation (PWM) carrier phase shift [11], have been applied to reduce torque ripples. However, torque ripples caused by back-EMF harmonics cannot be eliminated.

In this paper, a novel control scheme for non-sinusoidal back-EMF machines is proposed to obtain constant torques regardless of back-EMF waveforms. The proposed scheme is a combination of the classical FOC technique and a simple ADALINE. Thanks to self-learning and easy implementation, ADALINE is chosen in this study. Importantly, the ADALINE takes advantage of harmonic components in the torque to avoid the calculation burden, a long learning time, and highly fluctuating current references. Basically, these torque harmonics are multiples of the number of phases. The effectiveness of the proposed control scheme is shown by numerical results with a 7-phase PMSM drive. However, the proposed control scheme can be applied to every electric machine with an arbitrary number of phases and back-EMF characteristics, especially in real-time industrial systems.

This paper is organized as follows: modeling of a seven-phase machine will be described in section II; impacts of harmonic components of back-EMFs will be shown in section III; section IV is to describe control schemes; numerical results will be presented in section VI.

II. MODELING OF A 7-PHASE MACHINE

The following assumptions are considered to model the machine: seven phase windings of the machine are equally shifted and wye-connected; non-salient rotors are used; the 1st, 3rd, and 9th harmonics of back-EMFs account for highest proportions while other harmonics such as the 13th, 19th, and 11th are tiny but unneglectable; the magnetic circuit saturation is not considered in calculations of back-EMFs and fluxes. Thus, the voltage and electromagnetic torque can be expressed in natural frame as follows:

$$\underline{v} = R_s \underline{i} + [\mathbf{L}] \frac{d\underline{i}}{dt} + \underline{e} \quad (1)$$

$$T_{em} = \frac{\underline{e}^T \underline{i}}{\Omega} \quad (2)$$

$$\text{with } \underline{v} = [v_A \ v_B \ v_C \ v_D \ v_E \ v_F \ v_G]^T$$

$$\underline{i} = [i_A \ i_B \ i_C \ i_D \ i_E \ i_F \ i_G]^T$$

$$\underline{e} = [e_A \ e_B \ e_C \ e_D \ e_E \ e_F \ e_G]^T$$

where \underline{v} , \underline{i} , and \underline{e} are the 7-dimensional vectors of phase voltages, phase currents and back-EMFs, respectively; R_s is the resistance of the stator winding of one phase; $[\mathbf{L}]$ is the 7-by-7 stator inductance matrix; T_{em} is the electromagnetic torque of the machine; Ω is the rotating speed of the rotor. To facilitate the classical FOC technique, the classical 7-by-7 transformation matrices, Clarke $[\mathbf{T}]$ and Park $[\mathbf{P}]$, are applied to convert parameters of the machine from natural frame into decoupled d-q frames. For example, the transformation for currents is given by:

$$\underline{i}_{dq} = [\mathbf{P}][\mathbf{T}]\underline{i} \quad (3)$$

$$\text{with } \underline{i}_{dq} = [i_{d1} \ i_{q1} \ i_{d9} \ i_{q9} \ i_{d3} \ i_{q3} \ i_z]^T$$

where the selection of harmonic components of currents for control in each d-q frame depends on the main back-EMF harmonic in this frame. A 7-phase machine can be mathematically decomposed into 3 two-phase fictitious machines (FM1, FM2, FM3) and 1 zero-sequence machine (ZM) with corresponding decoupled reference frames (d_1 - q_1 , d_9 - q_9 , d_3 - q_3 , and z) [3]. A fictitious machine and its reference frame are associated with a given group of harmonics as described in TABLE I. As the wye-connected stator windings, zero-sequence current i_z in (3) is always equal to zero. Ideally, in the FOC-based control scheme, 6 constant d-q currents (i_{d1} , i_{q1} , i_{d9} , i_{q9} , i_{d3} , i_{q3}) can be simply controlled by six classical PI controllers.

According to the multi-reference theory presented in [3], a constant torque can be generated by constant d-q currents if each fictitious machine (FM1, FM2, or FM3) contains only one harmonic of back-EMF, for example the 1st, 9th, and 3rd harmonics. However, the imperfect machine design at low costs possibly results in undesired back-EMFs with more harmonic components. Without loss of generality, to see impacts of multi-harmonics in back-EMFs, it is assumed that there are two associated harmonics per reference frame as follows: the 1st and 13th associated with FM1 (d_1 - q_1); the 9th

TABLE I. HARMONIC CHARACTERIZATION OF FICTITIOUS MACHINES AND CORRESPONDING REFERENCE FRAMES (ONLY ODD HARMONICS)

| Fictitious machine | Frame | Associated harmonic $m \in \mathbb{N}_0$ |
|-------------------------------|---------------|--|
| 1 st machine (FM1) | d_1 - q_1 | 1, 13, ..., $7m \pm 1$ |
| 2 nd machine (FM2) | d_9 - q_9 | 9, 19, ..., $7m \pm 2$ |
| 3 rd machine (FM3) | d_3 - q_3 | 3, 11, ..., $7m \pm 3$ |
| Zero-sequence machine (ZM) | z | 7, 21, ..., $7m$ |

TABLE II. TORQUE RIPPLES GENERATED BY UNWANTED BACK-EMF HARMONICS IN FICTITIOUS MACHINES OF A 7-PHASE MACHINE.

| Fictitious machine | Current harmonics | Unwanted back-EMF harmonics | Harmonics in T_{em} |
|--------------------|-------------------|-----------------------------|-----------------------|
| FM1 | 1 | 13 | 14θ |
| FM2 | 9 | 19 | 28θ |
| FM3 | 3 | 11 | 14θ |

and 19th associated with FM2 (d_9 - q_9); the 3rd and 11th associated with FM3 (d_3 - q_3). The 11th, 13th, and 19th harmonics are called unwanted back-EMF harmonics in this study.

III. IMPACTS OF UNWANTED BACK-EMF HARMONICS

A. Impacts of unwanted back-EMF harmonics on current control

The impacts of unwanted harmonic components in back-EMFs on current control have been investigated in [4-6]. Indeed, unwanted back-EMF harmonics generate unwanted harmonics in d-q currents that low bandgap controllers such as PI cannot filter, resulting in low current control quality (unwanted harmonics in phase currents). Therefore, PI controllers combined with four ADALINES have been used for 5-phase machines. Meanwhile, six ADALINES with PI controllers have been applied to 7-phase machines. The effectiveness of the combination of PI controllers and ADALINES has been proven in transient and steady states. Therefore, the impacts of unwanted back-EMF harmonics are eliminated.

B. Impacts of unwanted back-EMF harmonics on torque generation

When unwanted harmonics in d-q currents are eliminated by using the above combination of PI controllers and ADALINES, all d-q currents are well controlled. In other words, phase currents only contain the imposed harmonics, for example 1st, 3rd, and 9th in the considered drive. However, torque ripples still exist. Indeed, the imposed current harmonics (1st, 9th, and 3rd) interact with unwanted back-EMF harmonics (13th, 19th, and 11th) to generate torque ripples with frequencies of 14θ and 28θ (θ is the electrical position) as described in TABLE II. Specifically, the torque in FM1 has a frequency of 14θ because the 1st harmonic of currents interacts with the 13th harmonic of back-EMFs. Similarly, torques in FM2 and FM3 have frequencies of 28θ and 14θ , respectively. Finally, the electromagnetic torque of the considered machine T_{em} , the sum of the three torques generated by the three fictitious machines, has frequencies of 14θ and 28θ . It is noted that these harmonic orders are multiples of the number of phases. By the same way, torque ripples at main frequencies of 6θ and 10θ can be observed in 3- and 5-phase machines, respectively. Therefore, these torque ripples need to be eliminated to guarantee smooth torques.

IV. TORQUE RIPPLE ELIMINATIONS

A. The vectorial approach

The vectorial approach in [7], known as maximum torque per ampere (MTPA), is to obtain constant torques regardless

of the presence of multi-harmonics in back-EMFs of multiphase machines. Current references in natural frame can be generally calculated as follows:

$$\underline{i}_{ref} = \frac{T_{em_ref} \Omega}{\|\underline{e}\|^2} \underline{e} \quad (4)$$

where \underline{i}_{ref} is the 7-dimensional vector of phase current references (natural frame); T_{em_ref} is the constant torque reference; $\|\underline{e}\|$ is the norm of the back-EMF vector \underline{e} in natural frame.

It is noted that current references in (4) are linearly proportional to back-EMFs. Therefore, when back-EMFs contains unwanted harmonics, currents in d-q frames are time-variant. Phase current references in (4) have been directly controlled by hysteresis controllers as in [7], resulting in inevitable variable switching frequencies, high switching losses, and electromagnetic compatibility problems. Similarly, highly oscillating current references are generated by the approach in [8] with ADALINE. For the sake of simplicity, the vectorial approach in [7] is used to compare with the proposed control scheme in this study.

B. Proposed control scheme with adaptive linear neurons

The principle of the proposed control scheme is to add compensating currents to the existing constant current references. These compensating currents are directly determined from harmonic components of the electromagnetic torque as described in TABLE II. Amplitudes of these torque harmonics depend on the back-EMF harmonic distribution. Meanwhile, phase angles of these torque harmonics depend on the drive (parasitic time delay, for example). These phase angles may change in the real-time operation of the drive. Accordingly, an additional torque, called compensating torque T_{em_com} , needs to be adaptively determined. This torque is expected to be equal to the difference between the constant torque reference T_{em_ref} and the electromagnetic torque T_{em} . To effectively determine the compensating torque, the control structure with only one ADALINE is proposed in Fig. 1. As previously discussed, the ADALINE is chosen because it possesses some advantages such as self-learning and easy-to-implement. The inputs of the ADALINE are harmonic components of the torque as described in TABLE II. The output of the ADALINE, the compensating torque T_{em_com} , is the weighted sum of the inputs as given by:

$$T_{em_com} = [w_{1_tor} \cos(14\theta) + w_{2_tor} \sin(14\theta)] + [w_{3_tor} \cos(28\theta) + w_{4_tor} \sin(28\theta)] \quad (5)$$

where (w_{1_tor}, w_{2_tor}) and (w_{3_tor}, w_{4_tor}) are weights of two harmonics 14θ and 28θ , respectively.

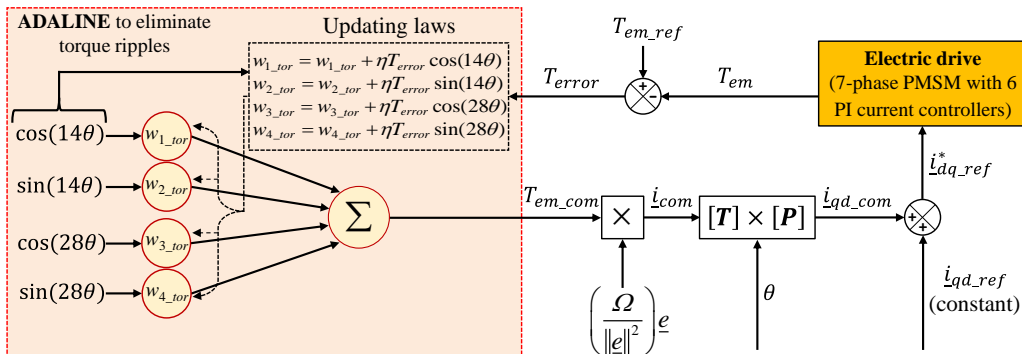


Fig. 1. The proposed control scheme using an ADALINE to eliminate torque ripples (implemented in the three rotating (d-q) frames).

In this study, Least Mean Square rule is applied to update these harmonic weights. In Fig. 1, the weights of harmonic components are updated by using learning rate η , corresponding harmonics (14θ and 28θ), and torque error T_{error} . The learning rate is required to be between 0 and 1 to guarantee the stability of the system. Its value depends on the input and output signals, and especially on the calculation power of processors used in the drive. Torque error T_{error} , the difference between torque reference T_{em_ref} and electromagnetic torque T_{em} , is given by:

$$T_{error} = T_{em_ref} - T_{em} \quad (6)$$

Thereafter, as introduced in [7], compensating currents in natural frame \underline{i}_{com} , calculated from compensating torque T_{em_com} in (5) and back-EMFs \underline{e} , can be expressed by:

$$\underline{i}_{com} = \frac{T_{em_com} \Omega}{\|\underline{e}\|^2} \underline{e} \quad (7)$$

The compensating currents \underline{i}_{com} are transformed into d-q frames \underline{i}_{dq_com} and added to constant current references \underline{i}_{dq_ref} . Then, the total current references $\underline{i}_{dq_ref}^*$ are used for control to create constant electromagnetic torques in the 7-phase drive. The total current references in d-q frames are no longer time-constant due to the compensating currents. It is worth noting that the proposed approach in Fig. 1 aims at learning only pulsating components of the torque to find compensating currents. Therefore, d-axis current references that do not generate torques are almost zero, facilitating current control with classical PI controllers. Meanwhile, the approach in [8] considers the entire torque reference in the learning process, resulting in highly oscillating d-q current references. Consequently, these d-q currents in [8] are like time-variant current references in [7]. Moreover, in the proposed control scheme, the ADALINE has only to find the amplitudes of considered harmonics instead of the entire harmonic signals. In other words, the knowledge of torque harmonics has been significantly used to reduce the number of calculations with therefore an expected short learning time. This proposed structure in Fig. 1 can be generally applied to every electric machine with different back-EMF characteristics and different numbers of phases. In those cases, torque harmonic components of which orders are multiples of the number of phases need to be determined.

V. NUMERICAL VERIFICATION

A. Parameters of the considered drive

The control schemes presented in the previous section are verified with MATLAB Simulink. Parameters of an experimental electric drive described in TABLE III are used

TABLE III. ELECTRICAL PARAMETERS OF THE 7-PHASE PMSM DRIVE.

| Parameter | Unit | Value |
|--|----------|-------|
| Stator resistance R_s | Ω | 1.4 |
| Self-inductance L | mH | 14.7 |
| Mutual inductance M_1 | mH | 3.5 |
| Mutual inductance M_2 | mH | -0.9 |
| Mutual inductance M_3 | mH | -6.1 |
| 1 st harmonic of the speed-normalized back-EMF | V/rad/s | 1.27 |
| 3 rd harmonic of back-EMF over 1 st harmonic | % | 32.3 |
| 9 th harmonic of back-EMF over 1 st harmonic | % | 12.5 |
| Number of pole pairs p | | 3 |
| Rated RMS current of the 7-phase PMSM | A | 5.1 |
| DC-bus voltage V_{DC} | V | 300 |
| PWM frequency | kHz | 10 |

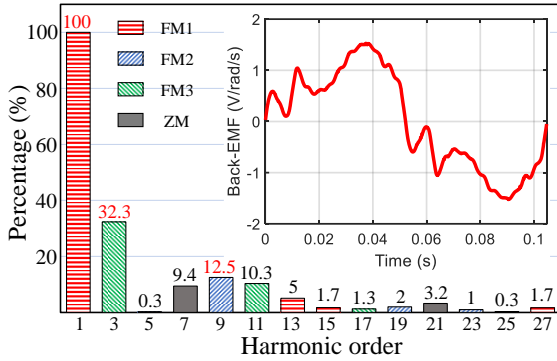


Fig. 2. Speed-normalized back-EMF and its harmonic spectrum of the considered 7-phase PMSM.

for simulations in this section. The 7-phase PMSM is supplied by a 7-leg voltage source inverter (VSI). The PWM strategy with a 3-level single-modulation is applied to generate switching signals of inverter switches at a frequency of 10 kHz. The 7-phase PMSM has a special concept. Specifically, this machine has an axial flux with double rotors. Different configurations of the double rotors result in several back-EMF waveforms. For example, when the two rotors have different numbers of poles and spatially shifted an angle of 7 degrees, the back-EMF waveform and its harmonic spectrum are presented in Fig. 2. Besides the 1st harmonic of the back-EMFs, the 9th and 3rd harmonics account for the highest proportions (12.5 and 32.3% of the 1st harmonic, respectively). Each of these harmonics presents in one fictitious machine. Several minor harmonics in fictitious machines can be described as follows:

1) *In FM1*: besides the 1st harmonic, the 13th harmonic is equal to 5% of the 1st harmonic.

2) *In FM2*: besides the 9th harmonic, the 19th harmonic is equal to 2% of the 1st harmonic, and approximately equal to 16% of the 9th harmonic.

3) *In FM3*: besides the 3rd harmonic, the 11th harmonic is equal to 10.3% of the 1st harmonic, and approximately equal to 32% of the 11th harmonic.

4) *In ZM*: the 7th and 21st harmonics are equal to 9.4 and 3.2% of the 1st harmonic. Due to the wye-connected stator windings, these harmonics have no effects on currents and torques.

B. Three operating stages for comparisons

To compare the vectorial approach and the proposed control scheme, an operation of the drive is considered with 3 stages as described as follows:

1) *Stage 1*: Time-constant d-q current references \underline{i}_{dq_ref} are used to generate an average torque equal to torque reference T_{em_ref} . Only three main harmonics of back-EMFs (1st, 9th, 3rd) are considered to calculate the current references by using (3)-(4). The classical FOC technique with 6 PI current controllers is applied.

2) *Stage 2*: Without changing the control scheme from stage 1, the vectorial approach in [7] is applied to define new d-q current references (time-variant), as calculated in (3)-(4), to theoretically generate constant torques. In other words, all harmonics of back-EMFs are used to calculate current references.

3) *Stage 3*: The proposed scheme in Fig. 1, a combination of the classical FOC technique and a simple ADALINE, is applied. In this case, compensating d-q currents are added to the constant d-q current references from stage 1 to obtain the total current references $\underline{i}_{dq_ref}^*$ for control.

C. Numerical results

Fig. 3 demonstrates the three operating stages at two speeds to see the effectiveness of the proposed control scheme in eliminating torque ripples. Specifically, torque, current control performances, and weight convergence are presented. Speeds of 10 rad/s and 40 rad/s are chosen due to the considered DC-bus voltage of 300 V. If the rotating speed is higher, the effectiveness of the proposed control scheme is more impressive over the vectorial approach. In Fig. 3, four weights (w_{1_tor} , w_{2_tor} , w_{3_tor} , w_{4_tor}) with a learning rate of 0.001 rapidly converge within one third of the electrical period or even faster. If the learning rate is increased, the convergence will be faster and vice versa but a higher overshoot even an instability may appear.

At a speed of 10 rad/s, stage 1 with a ripple of 10.7% at the main frequency 14θ as described in Fig. 3a. This ripple represents the impact of unwanted back-EMF harmonics on torque generation. In stage 2, new current references, created by using the vectorial approach in [7] and (3)-(4), generate a torque ripple of 1.7%. The torque is reduced to 1.2% by using the proposed control scheme as shown in stage 3. It is noted that the effectiveness of the proposed control scheme in stage 3 is not clear due to the low speed. Additionally, current references in stages 2 and 3 are not constant. Specifically, 6 d-q current references in stage 2 are time-variant with high amplitudes. Meanwhile, these currents of the proposed control scheme in stage 3 have much lower amplitudes, especially d-axis currents. This important characteristic affects current control quality at higher speeds. Indeed, at a speed of 40 rad/s, as shown in Fig. 3b, stage 3 using the vectorial approach has a ripple of 6.7% while the torque ripple in stage 3 is only 1.6%.

Phase currents in the three operating stages at 40 rad/s are shown in Fig. 4a. Current waveforms are like the back-EMF waveform (see Fig. 2). The root mean square (RMS) currents are similar in the three stages at about 5.1 A, the rated RMS current of the considered machine. Therefore, copper losses in the three stages are alike. However, a high peak phase current (11 A) can be seen in stage 2 while these currents in stages 1 and 3 are respectively equal to 9.2 A and 9.3 A. Phase voltage references at 40 rad/s are shown in Fig. 4b. It is noted that a high peak phase voltage (139.3 V) can be seen in stage 2 while these currents in stages 1 and 3 are respectively equal to 91.8 V and 106.5 V. In other words, the constant-torque region with the proposed control scheme will be larger.

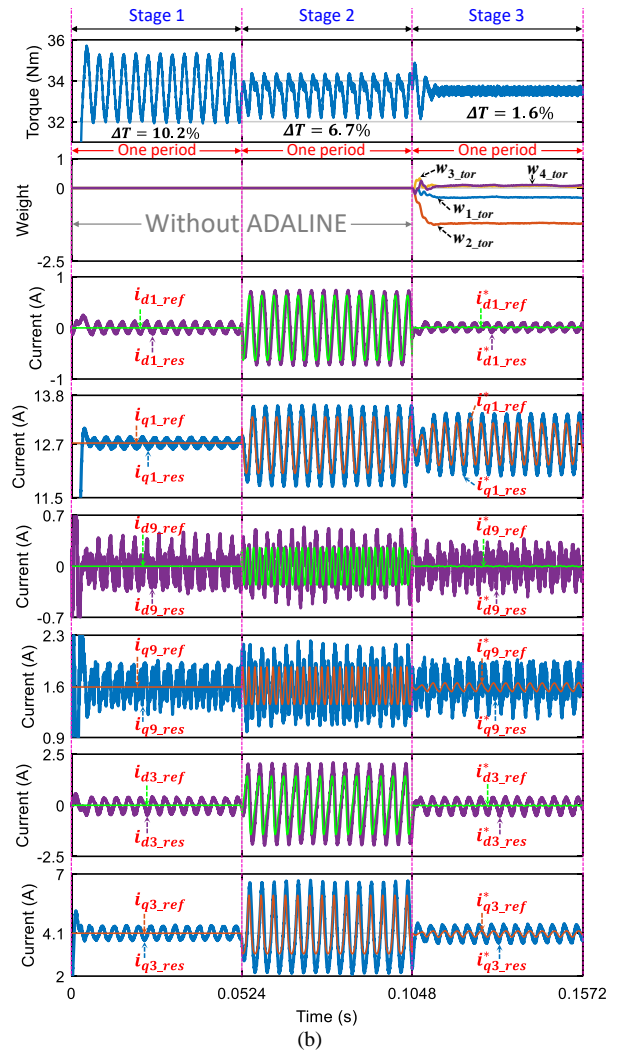
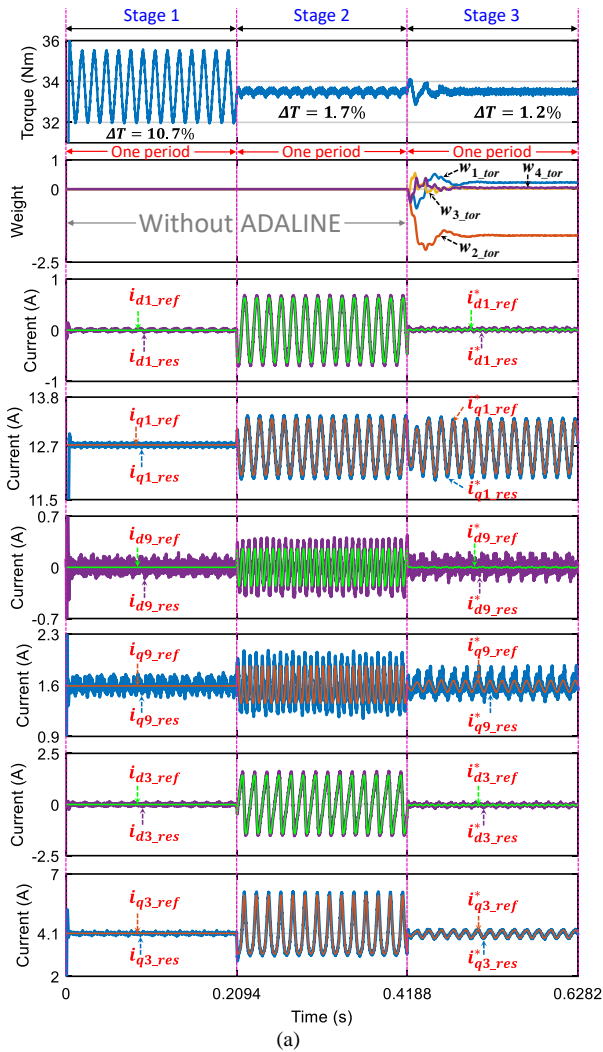


Fig. 3. With $T_{em_ref}=33.5$ Nm, torques, weights, and d-q currents in three operating stages at 10 rad/s (a), and at 40 rad/s (b), in which stage 1 considers constant d-q current references, stage 2 applies the vectorial approach with time-variant d-q current references, and stage 3 uses the proposed control scheme with ADALINE ($\eta=0.001$) (one period refers to one electrical period).

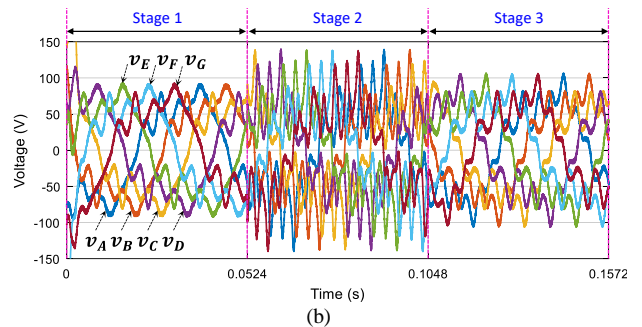
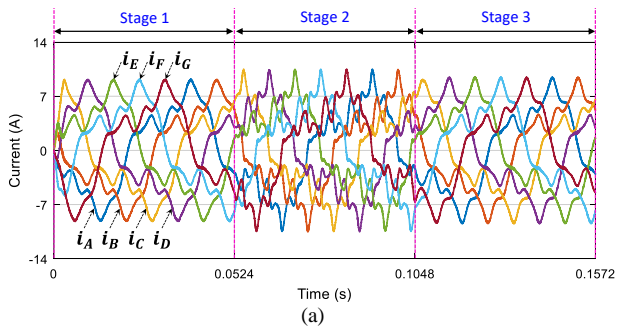


Fig. 4. At 40 rad/s with $T_{em_ref}=33.5$ Nm, phase currents (a), and phase voltage references (b) in the considered three operating stages in which stage 1 considers constant d-q current references, stage 2 considers the vectorial approach with time-variant d-q current references, and stage 3 uses the proposed control scheme with ADALINE ($\eta=0.001$).

Dynamic performances with variations of the rotating speed and torque reference are described in Fig. 5. The rotating speed suddenly varies from 10 to 25 rad/s and then returns to 5 rad/s in Fig. 5a. It is noted that the high torque quality is almost guaranteed at these different speeds when the torque ripple varies from 1 to 1.4%. In addition, the four weights converge within about one third of the electrical period even faster. When the rotating speed is fixed at 25 rad/s, the torque reference suddenly decreases from 33.5 to 13.5 Nm then goes up to 23.5 Nm as described in Fig. 5b. The torque ripple varies from 1.4 to 3.4%. The increase in the torque ripple is caused by the decrease in the average torque but not

by the control quality. The weights converge within one fifth of the electrical period even faster.

VI. CONCLUSIONS

In this paper, a generic control scheme for non-sinusoidal back-EMF of n -phase machines has been proposed and numerically verified with $n=7$. Thanks to the proposed control scheme, a low-cost machine with an imperfect back-EMF can generate constant torques. Especially, the classical FOC technique that is popular in industry continues to be used. Only a simple ADALINE is added. Thanks to self-learning, easy implementation, ADALINE has been chosen. Especially,

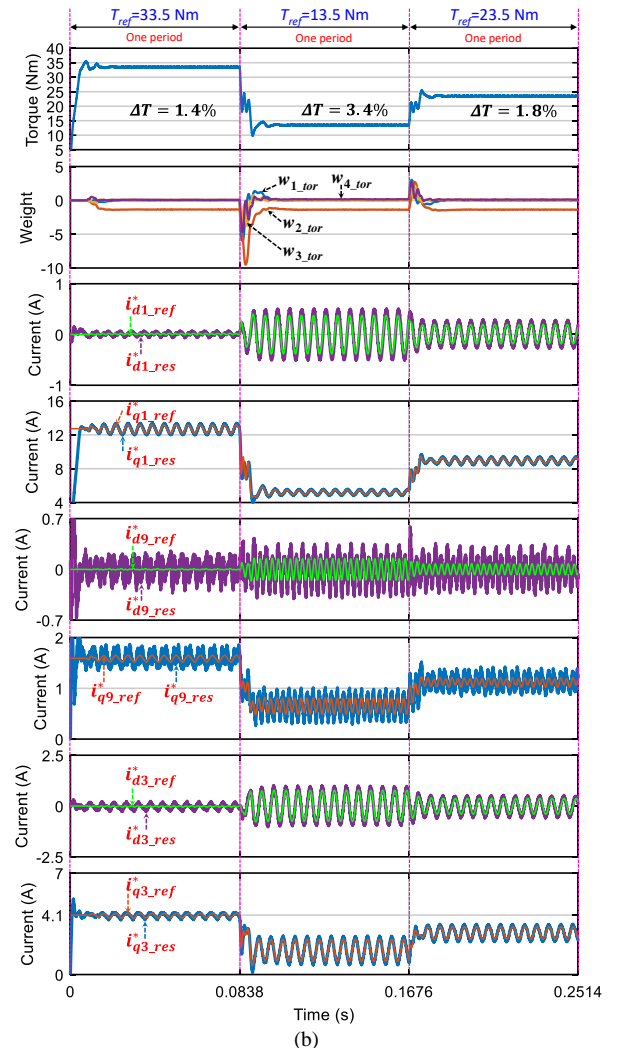
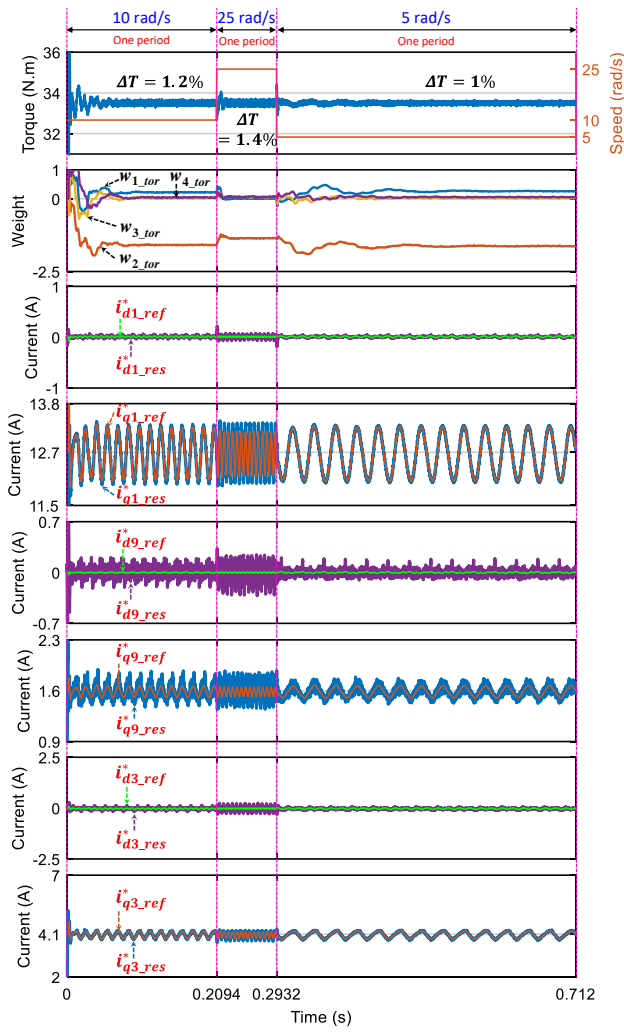


Fig. 5. Dynamic performances with the proposed control scheme using ADALINE with $\eta=0.001$ in terms of variations of the rotating speed with $T_{em_ref}=33.5$ Nm (a), and variations of the torque reference at 25 rad/s (b) (one period refers to one electrical period).

the use of knowledge of only torque harmonic orders $2n$ and $4n$ in a n -phase drive enables to reduce the calculation burden, enhancing the applicability of the proposed control scheme in real-time applications. Numerical results have proven the effectiveness and advantages of the proposed control scheme over the existing approaches.

ACKNOWLEDGMENT

This work has been achieved within the framework of CE2I project. CE2I is co-financed by European Union with the financial support of European Regional Development Fund (ERDF), French State and the French Region of Hauts-de-France.

REFERENCES

- [1] E. Levi, "Multiphase Electric Machines for Variable-Speed Applications," *IEEE Transactions on Industrial Electronics*, vol. 55, no. 5, pp. 1893-1909, 2008.
- [2] F. Barrero and M. J. Duran, "Recent Advances in the Design, Modeling, and Control of Multiphase Machines Part I," *IEEE Transactions on Industrial Electronics*, vol. 63, no. 1, pp. 449-458, 2016.
- [3] E. Semail, X. Kestelyn, and A. Bouscayrol, "Right harmonic spectrum for the back-electromotive force of an n -phase synchronous motor," in *the 39th IEEE Industry Applications Conference*, Seattle, WA, USA, 10/2004, vol. 1, pp. 71-78.
- [4] D. T. Vu, N. K. Nguyen, and E. Semail, "Eliminations of Low-frequency Current Harmonics for Five-phase Open-end Winding Non-sinusoidal Machine Drives applying Neural Networks," in *The 46th Annual*

- Conference of the IEEE Industrial Electronics Society (IECON)*, Singapore, 2020, pp. 4839-4844.
- [5] D. T. Vu, N. K. Nguyen, E. Semail, and T. T. N. Nguyen, "Current Harmonic Eliminations for Seven-phase Non-sinusoidal PMSM Drives applying Artificial Neurons," in *The International Conference on Engineering and Research Application (ICERA)*, Thai Nguyen, Vietnam, 2020, pp. 270-279.
- [6] L. Wang, Z. Q. Zhu, H. Bin, and L. M. Gong, "Current Harmonics Suppression Strategy for PMSM with Non-Sinusoidal Back-EMF Based on Adaptive Linear Neuron Method," *IEEE Transactions on Industrial Electronics*, pp. 1-1, 2019.
- [7] X. Kestelyn and E. Semail, "A Vectorial Approach for Generation of Optimal Current References for Multiphase Permanent-Magnet Synchronous Machines in Real Time," *IEEE Transactions on Industrial Electronics*, vol. 58, no. 11, pp. 5057-5065, 2011.
- [8] D. Flieller, N. K. Nguyen, P. Wira, G. Sturtzer, D. O. Abdeslam, and J. Mercklé, "A Self-Learning Solution for Torque Ripple Reduction for Nonsinusoidal Permanent-Magnet Motor Drives Based on Artificial Neural Networks," *IEEE Transactions on Industrial Electronics*, vol. 61, no. 2, pp. 655-666, 2014.
- [9] L. Guo and L. Parsa, "Model Reference Adaptive Control of Five-Phase IPM Motors Based on Neural Network," *IEEE Transactions on Industrial Electronics*, vol. 59, no. 3, pp. 1500-1508, 2012.
- [10] G. Li, J. Hu, Y. Li, and J. Zhu, "An Improved Model Predictive Direct Torque Control Strategy for Reducing Harmonic Currents and Torque Ripples of Five-Phase Permanent Magnet Synchronous Motors," *IEEE Transactions on Industrial Electronics*, vol. 66, no. 8, pp. 5820-5829, 2019.
- [11] X. Wang *et al.*, "Selective Torque Harmonic Elimination for Dual Three-Phase PMSMs Based on PWM Carrier Phase Shift," *IEEE Transactions on Power Electronics*, vol. 35, no. 12, pp. 13255-13269, 2020.